

## THE DENSITY JUMP ACROSS INTERNAL WORKING SURFACES IN HH JETS

A. C. Raga and J. Cantó

Instituto de Astronomía  
Universidad Nacional Autónoma de México

*Received 1998 May 29; accepted 1998 July 14*

### RESUMEN

Los nudos en algunos de los objetos Herbig-Haro (HH) han sido modelados exitosamente como “superficies de trabajo internas” que resultan de una variabilidad en la velocidad de eyección. La emisión de estos nudos parece estar casi siempre dominada por la emisión del choque a proa, o a lo más, con una pequeña contribución del disco de Mach. Como ha sido demostrado anteriormente, esto implica que la densidad del chorro en la dirección hacia la fuente es más alta que en la dirección opuesta. Este salto de densidad podría ser generado por el flujo mismo, o podría ser el resultado de una dependencia temporal de la densidad de eyección.

Estudiamos un modelo semi-analítico de la propagación de una superficie de trabajo interna. Con este modelo, demostramos que chorros eyectados con una velocidad variable sinusoidal (y con una densidad constante) siempre desarrollan fuertes saltos de densidad a través de sus superficies de trabajo internas. De este resultado, concluimos que los saltos de densidad observados pueden ser explicados en forma directa, sin recurrir a una variabilidad temporal de la densidad de eyección.

### ABSTRACT

Knots in some of the jet-like Herbig-Haro (HH) objects have been successfully modeled as “internal working surfaces” resulting from a time-variability of the ejection velocity. The emission from these knots appears to be almost invariably dominated by the emission from the bow shock, and has at most a small contribution from the jet shock (or Mach disk). As has been previously pointed out, this observational result implies that the flow upstream of the working surface is considerably denser than the downstream flow. This density jump could either be generated by the jet flow itself, or it might be the result of a time-dependence in the ejection density.

We study a simple, semi-analytic model for the propagation of an internal working surface. With this model, we show that jets ejected with a sinusoidal velocity variability (and with a time-independent density) always develop a strong up- to down-stream density jump across internal working surfaces. From this result, we conclude that the observed density jumps can be straightforwardly explained without recurring to a time-dependent ejection density.

**Key words:** HYDRODYNAMICS — SHOCK WAVES — STARS — FORMATION — STARS — MASS-LOSS

### 1. INTRODUCTION

Rees (1978) first suggested that a variability in the ejection velocity would result in the formation of travelling shocks which could produce the knot structures observed in astrophysical jets. Raga et al. (1990) argued that velocity variabilities of supersonic

amplitude would result in the formation of two-shock “internal working surfaces”, and tentatively identified the knots along Herbig-Haro (HH) jets with such structures. This model for knots in HH jets has subsequently been studied in some detail both analytically (Kofman & Raga 1992; Raga & Kofman 1992; Smith, Suttner, & Zinnecker 1997) and numerically

(Hartigan & Raymond 1993; Stone & Norman 1993; Gouveia dal Pino & Benz 1994; Falle & Raga 1993, 1995; Smith, Suttner, & Yorke 1997).

These models have recently become quite popular, as the *HST* images of some HH jets show that the resolved knots do morphologically resemble small internal working surfaces (e.g., HH 111; see Reipurth et al. 1997b). Also, the discovery of the “superjets” (see, e.g., Bally & Devine 1994; Ogura 1995; Devine et al. 1997; Reipurth, Bally, & Devine 1997a) implies that some of the well known HH objects (such as HH 34S or HH 111V), which have been interpreted in the past as the “heads” of jets, actually correspond to internal working surfaces.

This result directly raises the following question. It is observed in many HH objects (e.g., in HH 34S, HH 111V, HH 1) that the emission is dominated by the bow shock, and that there is, at most, only a small contribution from the jet shock (or Mach disk). As pointed out by Hartigan (1989), this implies that there is a high up- to down-stream density ratio across the working surface. If these working surfaces actually are internal to the jet beam, this implies that the jet beam is denser in the up-stream direction. Are we then seeing evidence for a time-dependence in the ejection density (as well as in the ejection velocity)?

It is not completely straightforward to see whether or not this is the case. It is clear that a jet ejected with a time-dependent velocity but time-independent density does develop a strong axial density profile (as seen, e.g., in the numerical simulations of Hartigan & Raymond 1993). Therefore, the observed up- to down-stream density ratio across internal working surfaces could actually be self-generated by the jet, and is not necessarily an indication of the presence of a time-dependent ejection density.

In order to study this problem, we first describe analytic expressions for a free-streaming flow and for the position and time at which a working surface is formed (§ 2). We then write a full equation of motion for the working surface (§ 3). Finally, we carry out a numerical integration of this equation of motion (§ 4), obtaining predictions of the properties of the working surface as a function of time (including a prediction of the up- to down-stream density ratio). The results are discussed in § 5.

Throughout this paper, we consider a simple, sinusoidal ejection velocity time-variability. Time-variabilities in stellar jet formation mechanisms have been studied in the past both in the context of purely gasdynamic (e.g., Kim & Raga 1991) as well as magnetohydrodynamic (Goodson, Winglee, & Böhm 1997; Ouyed & Pudritz 1997) mechanisms. However, these models are still in a somewhat primitive stage, and it is not even clear whether or not they can produce the timescales implied by the structures observed in HH jets. Because of this, we do not con-

sider a specific model for the ejection process, and arbitrarily only consider a sinusoidal time-variability. This variability can be interpreted as being a single Fourier component of an in principle more complex (but unspecified) ejection time-variability. For a description of jets ejected with a multi-mode time variability, we refer the reader to the paper of Raga & Noriega-Crespo (1998).

Finally, we should point out that we consider a purely gasdynamic jet (i.e., with no magnetic field). The presence of a magnetic field would introduce a considerably higher degree of complexity, which lies outside the scope of the semi-analytic model discussed in the present paper.

## 2. THE DEVELOPMENT OF INTERNAL WORKING SURFACES

Let us consider a hypersonic jet with a variable ejection velocity of the form

$$u_0(\tau) = v_0 + v_a \sin \omega \tau, \quad (1)$$

where  $\tau$  is the time at which the flow is ejected, and  $v_0$ ,  $v_a$  and  $\omega$  are constants. For high Mach numbers, the flow will be free streaming—except at the points in which discontinuities are formed, see Kofman & Raga (1992)—, so that it is described by the simple relations

$$u_0(\tau) = \frac{x}{t - \tau} = u(x, t), \quad (2a)$$

$$\rho(t, \tau) = \rho_0(\tau) \left[ 1 - (t - \tau) \frac{d \ln u_0}{d\tau} \right]^{-1}, \quad (2b)$$

where  $x$  is the distance from the source,  $t$  is the time and  $u(x, t)$  is the velocity along the flow axis. The second equation is valid for a constant cross section jet. In order to determine the density along the flow  $\rho(t, \tau)$ , it is of course necessary to specify the (time-dependent) density  $\rho_0(\tau)$  of the gas ejected by the source.

As discussed by Raga et al. (1990), internal working surfaces form at a distance  $x_c$  from the source, which is given by

$$x_c = \left[ \frac{u_0^2}{du_0/d\tau} \right]_{\min}, \quad (3)$$

where the minimum is taken over the whole phase of the ejection velocity variability. Using equation (1), from a simple analysis we find that the minimum is attained for

$$\tau_c = \frac{1}{\omega} \sin^{-1} \left[ \frac{1 - \sqrt{1 + 8(v_a/v_0)^2}}{2(v_a/v_0)} \right]. \quad (4)$$

From (1) and (3), we see that for our selected ejection velocity variability

$$x_c = \frac{v_0}{\omega} \frac{[1 + (v_a/v_0) \sin \omega \tau_c]^2}{(v_a/v_0) \cos \omega \tau_c}. \quad (5)$$

Finally, the time  $t_c$  at which the working surface forms is given by

$$t_c = \tau_c + \frac{1 + (v_a/v_0) \sin \omega \tau_c}{\omega (v_a/v_0) \cos \omega \tau_c}. \quad (6)$$

In order to visualize the implications of these equations, let us consider the case in which  $v_a \ll v_0$ . Keeping only terms linear in  $v_a/v_0$ , equations (4), (5) and (6) give

$$\tau_c \approx -\frac{2v_a}{\omega v_0}, \quad (7a)$$

$$x_c \approx \frac{v_0^2}{\omega v_a} \left[ 1 - 2 \left( \frac{v_a}{v_0} \right)^2 \right], \quad (7b)$$

and

$$t_c \approx \frac{v_0}{\omega v_a} \left[ 1 - 2 \left( \frac{v_a}{v_0} \right)^2 \right]. \quad (7c)$$

For very small  $v_a/v_0$ , from (7a) we see that the working surface is formed from material ejected at times  $\tau \approx 0$ , in the center of the  $u_0$  vs.  $\tau$  ramp of the sinusoidal velocity variation. For larger values of  $v_a/v_0$ , the working surface is formed from material ejected at more and more negative values of  $\tau$  (see [7a]). This has the interesting effect of breaking the symmetry between the regions up- and down-stream from the internal working surface.

### 3. THE PROPAGATION OF INTERNAL WORKING SURFACES

Once the internal working surface has formed, it travels downstream with the jet flow. If the working surface only traps a small amount of mass (between its two shocks), its motion is described by the simple, “ram pressure balance” equation

$$\frac{dx_{ws}}{dt} = v_{ws} = \frac{(\rho_l/\rho_r)^{1/2} u_l + u_r}{(\rho_l/\rho_r)^{1/2} + 1}, \quad (8)$$

where  $x_{ws}$  is the position and  $v_{ws}$  the velocity of the working surface,  $u_l$  and  $\rho_l$  are the velocity and density (respectively) directly upstream of the working surface, and  $u_r$  and  $\rho_r$  are the velocity and density (respectively) directly downstream. This situation is shown schematically in Figure 1. We should point out that equation (8) was given by Kofman & Raga

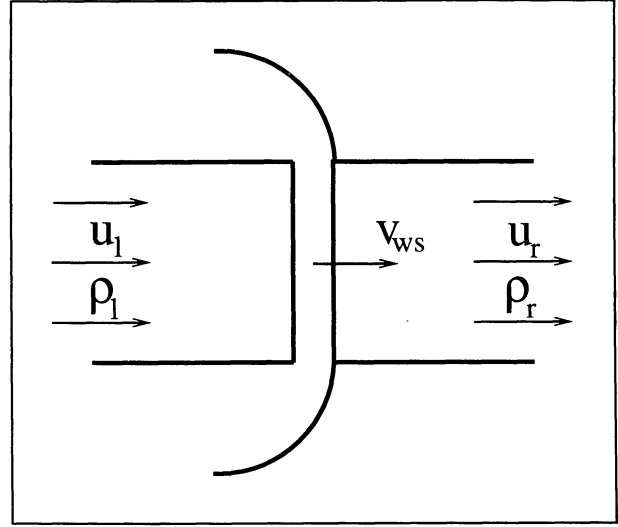


Fig. 1. Schematic diagram of an internal working surface. The working surface has two shocks formed by the interaction of the upstream material (with velocity  $u_l$  and density  $\rho_l$ ) with the downstream flow (with velocity  $u_r$  and density  $\rho_r$ ). The two-shock working surface moves away from the source with a velocity  $v_{ws}$ . Throughout the paper, we have assumed that the separation between the two working surface shocks is negligible. Also, there are two bow shock wings pushed into the surrounding environment. These bow shock wings are not considered in the present paper.

(1992), but also has been applied repeated times in the previous literature of astrophysical jets.

It is also possible to write an equation of motion for the working surface considering the inertia of the material trapped within the working surface shocks. However, as Raga & Kofman (1992) have shown, most of the mass intercepted by an HH jet working surface is ejected sideways, and does not pile up between the two working surface shocks. Because of this, equation (8) gives a realistic description of the motion of a working surface.

In order to integrate equation (8), the densities and velocities on the two sides of the working surface have to be specified. The velocities  $u_l$  and  $u_r$  can be straightforwardly determined by setting  $x = x_{ws}$  (in other words, assuming that the working surface has a negligible thickness), and finding the two relevant roots of equation (2a). These two roots give the values of  $u_l$  and  $u_r$  (and the corresponding ejection times  $\tau_l$  and  $\tau_r$ ). There is also a third, unphysical root with an ejection time  $\tau$  in between  $\tau_l$  and  $\tau_r$ . These roots have to be found numerically, because equation (2a) is transcendental for a sinusoidal ejection velocity variability (see equation [1]). The densities on the two sides of the working surface can be found by setting  $\tau = \tau_l$  or  $\tau = \tau_r$  in the solution for

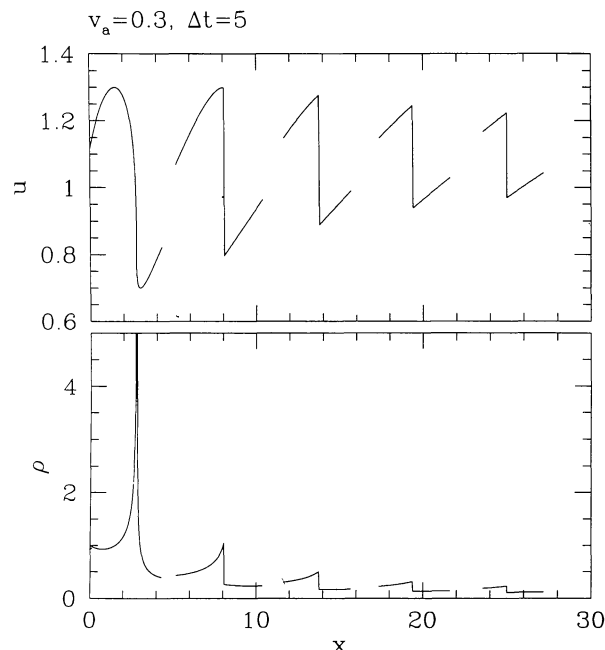


Fig. 2. Flow velocity (above) and density (below) for a model with  $v_a = 0.3$  (in units of the mean flow velocity  $v_0$ , see the text). The  $x$ -axis is the distance from the source measured in units of  $v_0/\omega$ . The velocity and density profile of the flow close to the working surface is plotted for 5 different times. The first profile corresponds to the time  $t_c = 2.747$  (in units of  $1/\omega$ , see equation [6]) at which the working surface is formed. The successive profiles correspond to  $\Delta t = 5$  time increments.

the density profile of a free streaming flow (equation [2b], also see Raga & Kofman 1992).

In order to obtain the time evolution of the working surface we then carry out a straightforward numerical integration of equation (8), with  $u_l$ ,  $u_r$ ,  $\rho_l$  and  $\rho_r$  determined by the auxiliary equations (2a) and (2b). The initial condition is  $x_{ws}(t_c) = x_c$ , where  $t_c$  and  $x_c$  are given by equations (4–6). The results of this numerical integration are described in the following section.

#### 4. NUMERICAL INTEGRATION OF THE MOTION OF AN INTERNAL WORKING SURFACE

We have carried out numerical integrations of the equation of motion of an internal working surface (described in the previous two sections). For sinusoidal ejection velocities (see equation [1]), by writing velocities in units of  $v_0$ , time in units of  $\omega^{-1}$  and positions in units of  $v_0/\omega$ , one has a one parameter family of the form  $u_0(\tau) = 1 + v_a \sin \tau$ . For our numerical simulations we furthermore assume that the ejection density has a constant value  $\rho_0(\tau) = 1$ . In

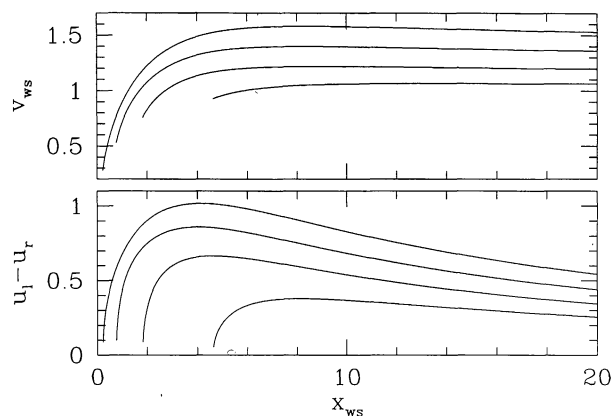


Fig. 3. Velocity  $v_{ws}$  of the working surface (top) and velocity jump  $u_l - u_r$  across the working surface (bottom) as a function of distance  $x_{ws}$  to the source. The curves correspond to solutions for  $v_a = 0.8$  (curve starting at the lowest  $x_{ws}$  value), 0.6, 0.4 and 0.2 (curve starting at the largest  $x_{ws}$  value). The curves start at the distance  $x_c$  at which the working surfaces are formed.

this way, we come up with a series of solutions which depend on the single parameter  $v_a$ , which can have values between 0 and 1.

The motion of the working surface obtained for  $v_a = 0.3$  is shown in Figure 2. In this figure we see the position of the working surface for different times (starting with the formation time  $t_c$ , see equation [6]), together with the flow velocity and density in the continuous flow regions to the two sides of the working surface. From this plot, it is clear that the flow directly upstream of the working surface is considerably denser than the downstream region for all times  $t > t_c$ .

Figure 3 shows the velocity  $v_{ws}$  of the working surface and the velocity jump  $\Delta v = u_l - u_r$  across the working surface as a function of distance  $x_{ws}$  from the source for solutions corresponding to  $v_a = 0.2, 0.4, 0.6$  and  $0.8$ . We find that  $v_{ws}$  initially grows with increasing  $x_{ws}$ , then reaches a maximum, and finally has a shallow decrease until it attains a constant value for large values of  $x_{ws}$ . The velocity jump  $u_l - u_r$  initially also grows, reaches a maximum, and decreases proportional to  $1/x_{ws}$  far away from the source (this is the asymptotic regime described by Kofman & Raga 1992).

Figure 4 shows the density ratio  $\rho_l/\rho_r$  and the shock velocity ratio  $v_{sr}/v_{sl} = (v_{ws} - u_r)/(u_l - v_{ws})$  between the two sides of the internal working surface (see the schematic diagram of Fig. 1). From these plots, we see that for all values of  $v_a$ , the upstream flow is always denser than the downstream flow (for all positions). The  $\rho_l/\rho_r$  ratio attains values of 10 and above in the solutions with  $v_a > 0.5$ .

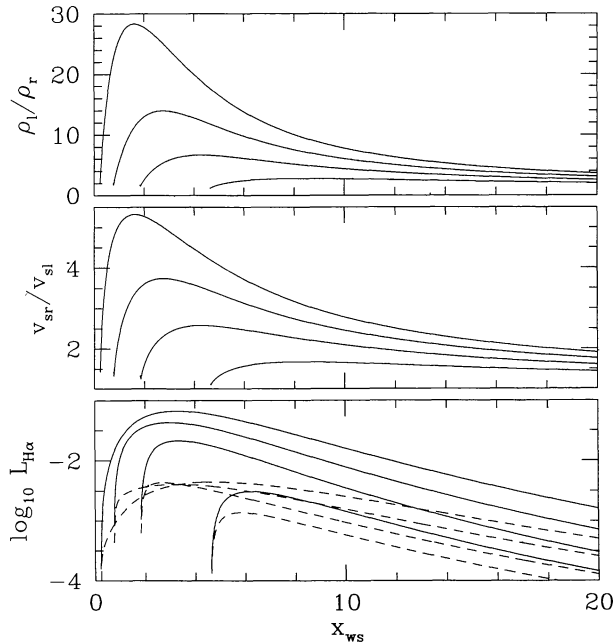


Fig. 4. Up- to down-stream density ratio (top), bow to jet shock velocity ratio (center) and dimensionless  $H\alpha$  luminosity of the bow (solid line) and jet (dashed line) shocks (bottom) as a function of the distance  $x_{ws}$  from the working surface to the source. The curves correspond to solutions for  $v_a = 0.8$  (curve starting at the lowest  $x_{ws}$  value), 0.6, 0.4 and 0.2 (curve starting at the largest  $x_{ws}$  value). The curves start at the distance  $x_c$  at which the working surfaces are formed.

Finally, in Fig. 4 we also show the  $H\alpha$  intensities for the two working surface shocks, calculated with the simple parametrization  $L_{H\alpha} = \rho_{pre} v_s^{3.8}$  derived by Kofman & Raga (1992). From this graph, it is clear that the downstream (bow) shock is always brighter than the upstream (jet) shock by a considerable amount, in qualitative agreement with observations of working surfaces in HH objects. Actually, using the ram pressure balance condition (see equation [8]),  $L_{H\alpha}(\text{bow})/L_{H\alpha}(\text{jet}) = (v_{sr}/v_{sl})^{1.8}$ , which from the results shown in Fig. 4 is always considerably greater than unity.

## 5. COMPARISONS WITH OBSERVATIONS

It would be interesting to carry out more quantitative comparisons between observations of HH objects and these predictions. At the present time this is somewhat difficult, because there are few clear observations of the Mach disk (or jet shock) emission.

The possibly most clear detection of a jet shock is in the HH 111V working surface (see the *HST* images of Reipurth et al. 1997b). Raga & Noriega-Crespo (1993) used the  $H\alpha$  and red [S II] fluxes of the bow

and jet shock of HH 111V (previously obtained by Reipurth, Raga, & Heathcote 1992) to deduce an up- to down-stream density ratio of  $\rho_l/\rho_r \approx 20$  for this working surface.

If we take this density ratio at face value, we would conclude that it could be reproduced with a sinusoidal ejection variability of amplitude  $v_a/v_0 \approx 0.6$ –0.8 (see Fig. 4), and with a time-independent ejection density. However, later work by Raga, Böhm, & Cantó (1996) has shown that there are possibly serious problems with the interpretation of the [S II] lines with the presently available shock models. Because of this result, we should consider the density ratio deduced by Raga & Noriega-Crespo (1993) with caution.

Another possible approach to deducing up- to down-stream density ratios across working surfaces is as follows. Heathcote & Reipurth (1992) measure the radial velocities directly up- and down-stream of HH 34S as well as the proper motion of this working surface. If we assume that the radial velocities correspond to the projections along the line of sight of  $u_l$  and  $u_r$  (see Fig. 1), and that the proper motion corresponds to the projection on the plane of the sky of  $v_{ws}$ , we can deproject the measured values and use equation (8) to calculate the density ratio  $\rho_l/\rho_r$  across the working surface.

The problem with this approach is that the HH 34 outflow lies quite close to the plane of the sky. Therefore, the de-projection of the radial velocities (necessary for obtaining  $u_l$  and  $u_r$ , see above) are strongly dependent on the assumed value for the orientation of the outflow. For example, if we take the  $\phi = 30^\circ$  angle (between the outflow axis and the plane of the sky) suggested by Heathcote & Reipurth (1992), we obtain a  $\rho_l/\rho_r \approx 60$  density ratio. If we consider the marginally lower  $\phi = 28^\circ$  value suggested by Eislöffel & Mundt (1992), we obtain a very different  $\rho_l/\rho_r \approx 5$  value. We therefore, conclude that given the uncertainty in the orientation angle of the outflow, it is not really possible to give a quantitative estimate of the up- to down-stream density ratio for this object. The uncertainties in the measured radial velocities and proper motions of course introduce even larger errors in the calculated density ratio.

From the above discussion, we see that even though it appears to be clear that in many objects an up- to down-stream density ratio substantially greater than unity is required by the observations, it is not possible to carry out a reliable determination of its value. More detailed studies of the kinematics and line ratios of the bow and jet shocks of working surfaces will be necessary in order to improve on this situation.

## 6. CONCLUSIONS

We have addressed the problem of why internal working surfaces in HH jets always appear to have a

bright bow shock and a faint jet shock (indicating a high up- to down-stream density ratio). In order to do this, we have written an equation of motion for the working surface, and the free-streaming density and velocity solutions for the contiguous jet beam segments.

We have assumed that the ejection velocity variability is sinusoidal, and that the ejection density is constant, so that we have a family of models which depend on the single parameter  $v_a/v_0$  (where  $v_0$  is the mean velocity and  $v_a$  the half-amplitude of the ejection velocity variability). From a numerical integration of the equations of motion, we find that for the chosen ejection variability we always have working surfaces (for all values of  $v_a$  and at all times) with up- to down-stream density ratios  $\rho_l/\rho_r > 1$ . This ratio is larger for the solutions with larger values of  $v_a/v_0$ .

From this, we conclude that internal working surfaces corresponding to large amplitude velocity variabilities will have large  $\rho_l/\rho_r$  values, so that their emission will be completely dominated by the emission from the bow shock. Fainter working surfaces (corresponding to variabilities with smaller amplitudes) will also be dominated by the emission from the bow shock, but the jet shock will not be as faint. For example, we predict that for a working surface with  $v_a/v_0 = 0.6$ , the bow shock will be brighter than the jet shock by a factor of  $\sim 10$  (see Fig. 4). For a working surface with  $v_a/v_0 = 0.2$ , the bow shock dominates over the jet shock by a factor of  $\sim 3$ .

Such an effect might be visible in the *HST* images of HH 111 (Reipurth et al. 1997b). In these images, the jet shock (i.e., the Mach disk) of the bright HH 111V working surface is not clearly discernible (becoming more apparent only on the  $H\alpha$ -[S II] line subtraction map). On the other hand, the smaller working surfaces closer to the source do seem to have clearly detectable jet shock emission. In order to quantify this effect, we plan to carry out a detailed comparison of these knots with numerical simulations in the future.

Finally, we would like to note that if HH sources have a time-dependent ejection velocity, they are of course also likely to have a time-dependent ejection density. With the simple calculations described in

this paper, we have shown that the density jumps observed across internal working surfaces in HH jets are reproduced (in a qualitative way) by a model in which the ejection density is constant. Therefore, the observed density jumps do not directly imply the presence of a strong ejection density variability. Such a variability, however, might still be present, but it will be necessary to carry out very detailed comparisons between observations and models in order to identify it.

## REFERENCES

- Bally, J., & Devine, D. 1994, *ApJ*, 428, L65  
 Devine, D., Bally, J., Reipurth, B., & Heathcote, S. 1997, *AJ*, 114, 2095  
 Eislöffel, J., & Mundt, R. 1992, *A&A*, 263, 292  
 Falle, S. A. E. G., & Raga, A. C. 1993, *MNRAS*, 261, 573  
 ——— 1995, *MNRAS*, 272, 785  
 Goodson, A. P., Winglee, R. M., & Böhm, K. H. 1997, *ApJ*, 489, 199  
 Gouveia dal Pino, E., & Benz, W. 1994, *ApJ*, 435, 261  
 Hartigan, P. 1989, *ApJ*, 339, 987  
 Hartigan, P., & Raymond, J. C. 1993, *ApJ*, 409, 705  
 Heathcote, S., & Reipurth, B. 1992, *AJ*, 104, 2193  
 Kim, S.-H., & Raga, A. C. 1991, *ApJ*, 379, 689  
 Kofman, L., & Raga, A. C. 1992, *ApJ*, 390, 359  
 Ogura, K. 1995, *ApJ*, 450, L23  
 Ouyed, R., & Pudritz, R. E. 1997, *ApJ*, 484, 794  
 Raga, A. C., Böhm, K. H., & Cantó, J., 1996, *RevMexAA*, 32, 161  
 Raga, A. C., Cantó, J., Binette, L., & Calvet, N. 1990, *ApJ*, 364, 601  
 Raga, A. C., & Kofman, L. 1992, *ApJ*, 386, 222  
 Raga, A. C., & Noriega-Crespo, A. 1993, *RevMexAA*, 25, 149  
 ——— 1998, *AJ*, in press  
 Rees, M. J. 1978, *MNRAS*, 184, 61P  
 Reipurth, B., Bally, J., & Devine, D. 1997a, *AJ*, 114, 2095  
 Reipurth, B., Hartigan, P., Heathcote, S., Morse, J. A., & Bally, J. 1997b, *AJ*, 114, 757  
 Reipurth, B., Raga, A. C., & Heathcote, S. 1992, *ApJ*, 392, 145  
 Smith, M. D., Suttner, G., & Yorke, H. W. 1997, *A&A*, 323, 223  
 Smith, M. D., Suttner, G., & Zinnecker, H. 1997, *A&A*, 320, 325  
 Stone, J., & Norman, M. L. 1993, *ApJ*, 413, 198

Jorge Cantó and Alejandro C. Raga: Instituto de Astronomía, UNAM, Apartado Postal 70-264, 04510 México, D.F., México (raga@astroscu.unam.mx).